Accepted Manuscript

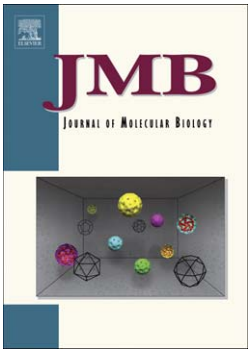

Structural biology and the design of new therapeutics: from HIV and cancer to mycobacterial infections

Sherine E. Thomas, Vitor Mendes, So Yeon Kim, Sony Malhotra, Bernardo Ochoa-Montaño, Michal Blaszczyk, Tom L. Blundell

PII: S0022-2836(17)30315-7
DOI: doi:10.1016/j.jmb.2017.06.014
Reference: YJMBI 65445

To appear in: *Journal of Molecular Biology*

Received date: 23 May 2017
Accepted date: 19 June 2017

Please cite this article as: Thomas, S.E., Mendes, V., Kim, S.Y., Malhotra, S., Ochoa-Montaño, B., Blaszczyk, M. & Blundell, T.L., Structural biology and the design of new therapeutics: from HIV and cancer to mycobacterial infections, *Journal of Molecular Biology* (2017), doi:10.1016/j.jmb.2017.06.014

This is a PDF file of an unedited manuscript that has been accepted for publication. As a service to our customers we are providing this early version of the manuscript. The manuscript will undergo copyediting, typesetting, and review of the resulting proof before it is published in its final form. Please note that during the production process errors may be discovered which could affect the content, and all legal disclaimers that apply to the journal pertain.

ACCEPTED MANUSCRIPT

Structural biology and the design of new therapeutics: from HIV and cancer to mycobacterial infections

A Paper Dedicated to John Kendrew

Sherine E. Thomas, Vitor Mendes, So Yeon Kim, Sony Malhotra, Bernardo Ochoa-Montaño, Michal Blaszczyk & Tom L. Blundell*

Department of Biochemistry, University of Cambridge

Tennis Court Road, Cambridge, United Kingdom

*corresponding author

Key words: Structure-guided; Fragment-based; Drug design/discovery; Cancer; Infectious disease; Mycobacterium.

Abbreviations: FBDD, fragment-based drug design; SPR, Surface Plasmon Resonance; NMR, Nuclear Magnetic Resonance; TB, tuberculosis; *Mtb, Mycobacterium tuberculosis; Mab, Mycobacterium abscessus; Mlep, Mycobacterium leprae;* HIV, Human Immunodeficiency Virus; AIDS, Acquired Immune Deficiency Syndrome; SAR, structure-activity relationship, non-tuberculous mycobacteria; NTM; dpCoA, 3'-dephospho Coenzyme A

ACCEPTED MANUSCRIPT

ACCEPTED MANUSCRIPT

ABSTRACT

Interest in applications of protein crystallography to medicine was evident as the first high-resolution structures emerged in the 50s and 60s. In Cambridge Max Perutz and John Kendrew sought to understand mutations in sickle cell and other genetic diseases related to haemoglobin, while in Oxford the group of Dorothy Hodgkin became interested in long-lasting zinc-insulin crystals for treatment of diabetes and later considered insulin redesign as synthetic insulins became possible. The use of protein crystallography in structure-guided drug discovery emerged as enzyme structures allowed the identification of potential inhibitor-binding sites and optimisation of interactions of hits using the structure of the target protein. Early examples of this approach were the use of the structure of renin to design anti-hypertensives and the structure of HIV protease in design of AIDS antivirals. More recently, use of structure-guided design with fragment-based drug discovery, which reduces the size of screening libraries by decreasing complexity, has improved ligand efficiency in drug design and has been used to progress three oncology drugs through clinical trials to FDA approval. We exemplify current developments in structure-guided target identification and fragment-based lead discovery with efforts to develop new antimicrobials for mycobacterial infections.

Early Development of Structure-guided Drug Discovery

When Max Perutz, John Kendrew and their colleagues in Cambridge were solving the first protein structures of myoglobin and haemoglobin in the 1950s and 60s[1-3], they were already aware of the importance of their work to medicine. Understanding the impacts of mutations on oxygen affinity and subunit cooperativity in abnormal haemoglobins that resulted in inherited single-gene disorders, such as sickle-cell disease, was recognised as a major objective. Dorothy Hodgkin's Oxford laboratory collaborated with Jørgen Schlichtkrull of Novo to understand how different crystalline forms of insulin could be exploited as slow-acting therapeutics for the treatment of diabetes[4]. This became a real possibility when the structure of insulin was solved[5, 6], as many insulin sequences had been defined in Fred Sanger's laboratory in Cambridge[7]. Sequences and structures stimulated ideas not only about insulin storage and receptor binding, but also about producing more effective therapeutics. These speculations became real opportunities when groups in Aachen, New York and Shanghai completed the synthesis of insulin, encouraging ideas about the design of novel synthetic insulins.

ACCEPTED MANUSCRIPT

Ideas about drug design were stimulated by the determination of the first enzyme structures – lysozyme, chymotrypsin and trypsin – in the 60s and an emerging understanding of the interactions that led to selectivity of enzyme substrate binding[8]. In the 70s and 80s, clinically important drug targets such as the aspartic protease renin[9, 10], which cleaves angiotensinogen to form angiotensin I, an essential step in regulating blood pressure, were modelled on less exciting enzymes such as fungal pepsins [11, 12]. The use of protein crystallography in drug discovery accelerated in the 1980s, especially by using a combination of protein structure and interactive computer graphics, such as the Evans and Sutherland machines[13]. The model of renin[14] was used widely in structure-guided drug design in the pharma industry in the 1980s. The high-resolution X-ray structures of apo-enzymes and complexes of renin and its close homologues followed much later[15, 16].

New Paradigm of Structure-guided Drug Discovery: Targeting HIV Protease

Probably the most influential development was the design of AIDS antivirals, based on the structure of HIV protease; these moved onto the market very quickly in the 1990s. Some basic science influenced this! In 1978, Jordan Tang who had sequenced pepsin together with crystallographic collaborators suggested that proteases had evolved from an ancestral dimer by gene duplication, fusion and divergence to give more effective enzymes[17]. A close relative of this dimeric ancestral aspartic protease was found in the retroviral proteases, first in Rous Sarcoma Virus, but then in HIV soon after the AIDS epidemic was recognised in the US and Europe. The genome of HIV, which encodes a polyprotein, was shown to include a protease[18], which was quickly recognised as a dimeric viral protease essential for the generation of infectious viral particles, and a model was produced based on the aspartic proteinase evolutionary relationship[19]. In 1989 structures followed for Rous Sarcoma Virus [20, 21] and HIV protease[22, 23], the structure of which was improved by further experimental structures determined independently by two labs[24] [25]. The subsequent development of new AIDS antivirals by 1997, including four very successful drugs (Roche Pharmaceuticals' saquinavir, Abbot's ritonavir, Merck's indinavir, and Agouron's nelfinavir) demonstrated the importance of understanding the genome not only in terms of functions of gene products, but also their architectures for use in structure-guided drug discovery, recorded recently in an excellent history of macromolecular crystallography and its fruits[26]

ACCEPTED MANUSCRIPT

The identification of HIV protease as a target and the development of AIDS antivirals was a new paradigm in drug discovery. It demonstrated that there was value in computational analysis of genomes in order to identify targets. This was an "exploration of biological space", an exciting challenge in the early 1990s as the sequence determination of human infectious agents such *Mycobacteriaceae* that give rise to tuberculosis and leprosy, as well as the very much larger genome of *Homo sapiens* became real prospects. The HIV protease inhibitor story also illustrated the importance "exploring chemical space": using protein structure to estimate the druggability of potential targets, followed by exploration of possible binding using screening libraries of chemical compounds. This idea of drug discovery can be summarised, as in Figure 1A.

Over the subsequent 25 years, several new approaches have been introduced that exploit knowledge of the architecture of the target and screening of chemical libraries. One of the most influential has been the development of structure-guided fragment-based drug discovery.

Protein Crystallography, Fragment-Based Drug Discovery and Oncology

In the 1980s and 90s meeting the challenge of the size and diversity of "chemical space" became a focus in the pharmaceutical industry with the realisation that chemical libraries of several thousand drug-like compounds explored only a tiny area of the chemical space. In order to estimate the number, Lipinski rules assuming a molecular weight limit of 500 daltons, the presence of carbon, hydrogen, oxygen, nitrogen and sulfur, and a maximum of 4 rings leads to an estimate of 10^{63}[27]. Big pharma searched the world for new chemical diversity, often using the products of our natural environment in underdeveloped-forested areas. The chemical libraries grew to hundreds of thousands of compounds and screening was roboticized to cope with the challenge. But a solution to the challenge was also found in a different approach in which complexity of the chemicals screened was reduced by decreasing their molecular weights, which at the same time increased their promiscuity in binding targets. The innovation that allowed decrease of size of the chemical screening library was fragment-based drug discovery (FBDD).

In FBDD, a fragment library often of ~ 1000 compounds of <300 Da is screened against the target of interest, resulting in identification of initial hits. These are then moved to lead candidates by chemically growing or linking the fragments followed by optimisation of interactions, thereby exploring the chemical space available for binding to the target protein very effectively. A high-affinity lead molecule thus

ACCEPTED MANUSCRIPT

developed from a fragment hit retains the key binding interactions of the original fragment with the "hotspot" on the target protein. Most of the fragments have lower potency than the more complex molecules found in typical high-throughput screening (HTS) compound libraries, however small fragments that bind, do so by making well defined and directional high-quality interactions and by displacing unhappy water molecules at the hotspots, giving rise to high ligand efficiency[28].

Early experiments used ligand-based NMR (Steve Fesik and his colleagues at Abbott) [29] and X-ray crystal screening[30, 31], developed at Astex initially by exploiting high-throughput analysis of cocktails of six to ten fragments soaked into apo-protein crystals. Knowledge of the structure of the complex of the fragment with target protein allowed the initial use of small, often non-chiral compounds, which were optimized using structure-guided approaches to make specific interactions and to introduce chirality in the molecules. The resulting fragment hits were capable of achieving high binding efficiency per atom and often better physicochemical properties in comparison to those from HTS approach which exploits much larger libraries of ~10^6 or more compounds[30, 32].

The relatively low affinities mean that a combination of biochemical, biophysical and structural techniques must be used to monitor hit identification, validation and subsequent elaboration into lead molecules, as summarised in Figure 1B. The choice of methods will depend on factors such as the availability of a sensitive biochemical assay, the solubility and stability of the protein, the existence of crystals of the apo-protein, and so on. Many groups use a two-stage approach of high-throughput screening of the fragment library using fluorescence-based thermal shift measurements[32, 33], ligand-based NMR, surface plasmon resonance (SPR) and increasingly with the roboticized screening facilities available on synchrotron beamlines, X-ray crystallographic screening. The fragment hits common between these techniques are then validated by optimisation of resolution of the structures by X-ray diffraction or structure determination by NMR if not possible to define by X-ray methods, as well as defining the kinetics with SPR and the thermodynamics of the binding using isothermal calorimetry. The combination of these techniques and others (Figure 1B) gives reassurance of the quality of the hit. The validated fragment hits are then elaborated iteratively by growing to a larger molecular weight or by linking using structure-guided techniques.

Where a crystal structure is not available, several labs have used fragment libraries to search chemical space using methods such as SPR[34], sometimes with many thousands of chiral compounds, often derived from analysis of successful drugs[35].

ACCEPTED MANUSCRIPT

Where an experimental structure or computational homology model is available, the pipeline can be complemented by substructure searches on commercially available compound databases or *in-silico* screening predictions of analogues[36, 37]. An example of this approach was that of Winter *et al.* [38], who had no suitable crystal structure to identify hits that disrupt the interaction between hepatocyte growth factor/scatter factor N-terminal fragment and the hepatocyte growth factor receptor (Met), and subsequently inhibit Met signalling. They carried out sub-structure searches on initial hits identified by biophysical methods such as SPR, and followed these by *in-silico* docking predictions to identify compounds, with significant anti-tumorigenic and anti-migratory activity in cell-based assays.

In 2011 the first fragment-derived drug, Vemurafenib, was approved targeting a mutant form of BRAF, extending life for patients with skin cancer. The drug was discovered at Plexxikon and developed in partnership with Roche. The second drug, Venetoclax, developed by AbbVie and Genentech, binds to BCL-2 and blocks its interaction with other proteins; was approved by the US FDA in 2016 for chronic lymphocytic leukemia (CLL). In 2017 the third drug, Ribociclib, by Astex and Novartis was approved for targeting the protein kinase Cdk4 and will be used in combination with letrozole as a first-line treatment for advanced breast cancer. All of these campaigns featured an important role for structure-guided approaches with a combination of activity in relatively small companies, often founded by academics with an interest in protein structure, but developed as cancer therapeutics with strong scientific and financial involvement of large pharma.

Moving Structure-guided Discovery from Oncology to other Diseases

We have shown that the HIV protease paradigm exploiting a combination of efficient exploration of biological space by understanding the genome and structural proteome, together with exploration of chemical space using structure-guided and fragment-based approaches, works well in cancer. As described above, FBDD has not only provided useful leads but also led to drugs that have been approved by the FDA. Much of the work has been done in biotech and small pharma companies in collaboration with large pharma.

We now address the question as to how far this structure-guided approach can be used to target diseases that are rare in the West, where big pharma finds it more difficult to get returns on its investment. These include genetic diseases occurring in a few families, for example cystic fibrosis or black bone disease (alkaptonuria), or those

ACCEPTED MANUSCRIPT

infectious diseases that are mainly found in developing countries, such as tuberculosis and leprosy. Large pharma finds these diseases more challenging to address, as the financial returns on investment are limited either by the small numbers of patients or by the difficulty in finding a market in relatively less prosperous countries in Africa, South America and the Indian subcontinent.

Structure-guided approaches will depend on knowledge of the genomes and strain variation of the causative organism in order to develop a fruitful/successful target-based approach. This is being addressed worldwide, mainly by charitable initiatives such as the Wellcome Trust at their Genome Campus or the Bill & Melinda Gates Foundation in initiatives such as HIT-TB and Shorten-TB. There is also considerable activity in Government-funded institutes such as NIH as well as academia, for example the London School of Hygiene and Tropical Medicine in the UK. Some companies, such as GlaxoSmithKline, have active research programmes in infectious disease, while several are involved with academic institutions in the TB Drug Accelerator (TBDA) partnership, supported by the Bill &Melinda Gates Foundation.

Here we focus on infectious diseases caused by mycobacteria to illustrate the way that structure-guided lead discovery in academia can use its experience in early lead discovery built on biochemistry, medicinal chemistry and structural biology, together with microbiology and human medicine. We show how knowledge of protein structure is central not only to select targets (exploring biological space) but also to develop new leads (exploring chemical space).

Genomes of *Mycobacteriaceae*

The *Mycobacteriaceae* family comprises 174 known species of acid-fast bacteria with high GC content and much thicker hydrophobic outer cell walls (containing mycolic acids) than most other bacteria [http://www.bacterio.net/mycobacterium.html]. The family includes several pathogenic bacteria such as *Mycobacterium tuberculosis* (*Mtb*, the causative agent of tuberculosis), *Mycobacterium leprae* (*Mlep*, causes leprosy), *Mycobacterium abscessus* (*Mab*, rapid-growing opportunistic pathogen that causes chronic lung diseases) and free-living non-pathogenic bacteria such as *Mycobacterium smegmatis*.

Mtb, found in *Homo sapiens*, is an obligate pathogen, which has evolved with humans over many thousands of years. According to the most recent WHO report, 10.4 million people were diagnosed with tuberculosis (TB) and 1.4 million died because of the infection in 2015, and an additional 0.4 million TB deaths have been reported among

ACCEPTED MANUSCRIPT

HIV-positive patients (WHO global TB reports 2016) [39]. Current first-line therapy for drug-sensitive TB involves a combination of four drugs (isoniazid, rifampicin, pyrazinamide and ethambutol) for two months followed by four months of a combination of isoniazid and rifampicin. The rise of multi-drug resistant TB (MDR-TB) and extensively drug resistant TB(XDR-TB) further necessitates prolonged therapy and the addition of second and third line antibiotics such as aminoglycosides, fluoroquinolones and macrolides. These drugs are often poorly tolerated, ineffective against drug-resistant TB or have toxic side effects due to the required prolonged treatments (up to 24 months), thereby leading to significant morbidity and mortality[40].

Although previously thought to be benign environmental microbes, Non-Tuberculous mycobacteria (NTM) are increasingly observed over the past decade, as a cause of infections worldwide[41, 42]. This paradigm shift in NTM prevalence is presumably due to higher environmental exposure rates to such mycobacteria, increased selective pressure imparted by intensive antibiotic use in patients, autophagy-inhibition-associated reduction in host immunity after prolonged antibiotic treatment or patient-to-patient transmission[43, 44]. *Mab*, a distant relative of *Mtb* and *Mlep*[45, 46]is a free-living nontuberculous mycobacterium commonly found in water and soil, which causes skin and soft-tissue infections and pulmonary diseases, particularly in patients with lung disease (such as cystic fibrosis) or a previous history of tuberculosis[47, 48]. A single-centre retrospective study of CF patients showed an increase in incidence of NTM infections from 0 to 9% over a period from 2002 to 2011[49].

After several changes in nomenclature and subspecies differentiation over recent years, the *M.abcessus complex* is now considered to comprise three distinct subspecies: *M.abcessus subsp. abscessus, M.abcessus subsp. massiliense and M.abcessus subsp. bolletii* [47, 50, 51]. High virulence and resistance to chemotherapy of *Mab complex* is attributed to a combination of intrinsic and acquired resistance mechanisms. The intrinsic resistance of *Mab* and other mycobacteria to drugs results from factors such as low permeability of the mycobacterial cell envelope acting synergistically with antibiotic inducible internal systems like drug-efflux pumps, antibiotic-inactivating enzymes, target-modifying enzymes and genes providing metal resistance [52-54]. Acquired resistance is frequently associated with spontaneous mutations of antibiotic target genes, although alteration in function of one or more other genes may also be involved[52, 53].

The current clinical management of *Mab* infection in CF is highly challenging due to the high rates of resistance of the bacterium to antibiotics and most of the classical

ACCEPTED MANUSCRIPT

anti-tuberculosis drugs[45]. Further, owing to its resistance to most commonly used disinfectants, various outbreaks of *Mab* infections in clinical and post-surgical settings have been reported[55]. Current treatment involves prolonged therapy using antibiotic combinations such as clarithromycin, amikacin, and cefoxitin, which are often poorly tolerated and lead to toxic side effects[47]. Hence, there is an urgent need of effective drugs to treat *Mab* infection.

For the *Mab* proteome there are greater challenges, due to the poor annotation of the *Mab* genome leading to 4920 predicted protein coding sequences[54], nearly one thousand more than for *Mtb* (3959 coding sequences), and the availability of only 39 experimentally defined structures in the Protein Data Bank (PDB)[56, 57]. A preliminary modelling exercise has predicted structures of over 3000 of these genes[58] & [Malhotra, S & Blundell, TL: unpublished].

Fragment Screening for *Mycobacterium abscessus*

Our approach to lead discovery for *Mab* targets has been centred on the experience gained with the Gates Foundation HIT-TB and EU-FP7 MM4TB *Mtb* programmes. To develop the *Mab* fragment-screening programme it was fundamental to identify essential gene products in this organism that have either a known crystal structures or alternatively an orthologue of a known structure, where we already had an *Mtb* FBDD programme. This strategy led to targeting PurC (SAICAR synthase), an enzyme involved in bacterial *de-novo* Purine biosynthesis and TrmD (tRNA-(N^1G37) methyl transferase), an essential tRNA modifying enzyme in bacteria, by reproducing the known *Mab* 3D structures, and selecting CoaD/PPAT (Phosphopantethiene adenylyl transferase), where we had a programme for *Mtb* funded by the Gates Foundation HIT-TB.

Phosphopantetheine adenylyltransferase (PPAT) catalyzes the penultimate step in the biosynthesis of CoA in prokaryotes. Coenzyme A (CoA), an essential co-factor for many cellular enzymes involved in biosynthetic, degradative and metabolic pathways, acts as an important acyl group carrier for all organisms[59]. The biosynthesis of CoA consists of a five-step reaction catalysed by different enzymes and utilizing pantothenate (Vitamin B5), cysteine and ATP[60] as starting substrates. PPAT enzyme is a member of the nucleotidyltransferase α/β phosphodiesterases superfamily and catalyses the reversible transfer of an adenylyl group from ATP to 4'-phosphopantetheine (Ppant) to yield 3'-dephospho-CoA (dPCoA) and pyrophosphate,

ACCEPTED MANUSCRIPT

as shown in Figure 2A. dPCoA in turn is phosphorylated by dephospho-CoA kinase (DPCK) to generate CoA[61, 62].

Although some bacteria are capable of *de novo* pantothenate synthesis, others utilize extracellular pantetheine for the biosynthesis of CoA. Nonetheless, all intermediate pathways converge at the penultimate step of CoA biosynthesis catalysed by PPAT[63]. Studies of CoA pathway intermediates in *Escherichia coli* showed that pantothenate and 4'-phosphopantetheine (Ppant) accumulated in the cell, suggesting an important rate-limiting role of PPAT in the pathway that may be crucial to its potential as an antibiotic target[63-65]. In higher eukaryotes, the final two steps of CoA biosynthesis are catalysed by a single bi-funtional enzyme called CoA synthase, containing a PPAT like domain. The marked structural differences between bacterial and human PPATs further suggest the potential for this bacterial enzyme as a novel antibiotic target[66-68].

The previously determined PPAT structures from various bacterial species such as *Escherichia coli, Staphylococcus aureus, Pseudomonas aeruginosa, Enterococcus faecalis, Burkholderia pseudomallei* and *Mab* demonstrate the presence of a canonical Rossmann fold as seen in many dinucleotide binding proteins. Attempts to develop PPAT inhibitors targeting *E-coli* PPAT enzyme, using HTS and combinatorial synthesis were only partially successful as none of the resulting candidate compounds showed inhibitory activity at the cellular level[69, 70]. A high throughput screening of the AstraZeneca compound library and subsequent structure-guided lead optimization led to the development of a set of compounds that significantly reduced the bacterial burden of gram-positive bacteria such as *S. pneumoniae* and *S. aureus* both *in vitro* and in animal models of infection[71]. However, these compounds were not progressed into clinical development owing to unfavorable toxicity and pharmacokinetic profiles.

We have built on the fragment-based drug discovery campaign against *Mtb* PPAT, which has led to the development of potential lead compounds having binding affinities to *Mtb* PPAT in the low micromolar range (Jamal, E. B., Blaszczyk, M., Blundell, T.L. & Abell, C. unpublished). We solved the crystal structures of *Mab* PPAT in apo form (PDB code*:* 5O06), and in a binary complex with the enzyme product, *3'*-dephospho Coenzyme A (PDB code*:* 5O08). Having a working crystallization system, we then initiated a structure-guided fragment-based drug discovery campaign against *Mab* focused on this target.

The crystal structure shows that the biologically active hexameric form of *Mab* apo-PPAT consists of two trimers, as seen with all known PPATs from bacteria[72-77].

ACCEPTED MANUSCRIPT

Each subunit consists of a canonical Rossmann fold[78] made of five parallel β-strands surrounded by six α-helices (Figure 2B & C).

The three-dimensional structure of *Mab* PPAT in complex with the reaction product, 3'-dephospho Coenzyme A (dpCoA) shows a similar binding mode to the one previously observed for *Mtb* PPAT, where dpCoA binds to all six sub-units of the hexamer[79]. The reaction product spans the large active-site cavity of *Mab* PPAT and adopts a 'bent' conformation upon binding, as has been previously observed with PPAT: dpCoA structures from other bacterial species[72-77] (Figure 2C & D).

A structural superposition of *Mab* PPAT:Apo and *Mab* PPAT:dpCoA shows large conformational changes in the flexible loop II (residue range 36-46) that connects β-strands β2 and α-helix α2 as well as loop IV (residues 87-99) at the base of the active site (Figure 2D & E). In *Mab* PPAT:dpCoA structure, loop II is found to have shifted towards the active site by about 7Å, when measured at Cα atom of Lys41, as compared to its position in *Mab* PPAT:Apo structure (Figure 2D & E). This large shift in loop II positions the invariant catalytic Lys41 residue favorably within H-bonding distance of adenylate α-phosphate (2.8 Å) and 4'-phosphate (2.9Å) of dpCoA respectively.

The initial fragment screening of the Cambridge in-house library, consisting of 960 fragments, was performed on *Mab* PPAT, using differential scanning fluorimetry. Thirty fragments from the library showed a difference in unfolding temperature greater than 1^{o}C upon PPAT binding. For the validation of these fragment hits, the structure of each was investigated by X-ray crystallography, resulting in crystal structures of PPAT in complex with fragments at resolutions ranging from 1.4 to 1.9 Å for 18 out of 30 fragment hits studied. The fragments were found to occupy four distinct binding sub-pockets within the PPAT active site, as shown in (Figure 3C & D). These fragments included examples that occupy the binding sites for adenylyl and 4'-phosphopantetheine regions of dpCoA, thereby spanning the entire active site groove of PPAT. Sub-pockets **I** & **II** correspond to the indole and ribose phosphate binding regions of dpCoA respectively whereas **III** & **IV** correspond to pantothenate and β-mercaptoethylamine sites of dpCoA respectively. Binding of fragments is mediated by several strong and weak hydrogen bonds, π-interactions as well as hydrophobic and ionic contacts. Figure 4 shows the detailed binding mode of 6 representative fragment hits at sites **I** to **IV**.

ACCEPTED MANUSCRIPT

Many fragments engage key residues, such as His17, Arg90, Val125, Ser9, Leu73 involved in substrate binding and transition state stabilization of PPAT[72], in addition to making new interactions. Fragments binding to sites **I** & **II,** for example, mimic some of the strong π-interactions to side chains of Arg 90 and His 17 and hydrogen bonding interactions to the back bone amide of Gly 88, mediated by the adenylyl part of dpCoA (Figures 3A & 4). PPAT binding to dpCoA was found to result in considerable ordering and rearrangement of the loop IV to two complete α-helical turns at the N-terminal of helix4. Several fragments also lead to a similar conformational switching of loop IV near the base of the catalytic site of PPAT as shown in Figures 2E & 3B. Fragments at site **III** and **IV** recapitulate interactions of 4'-phophospantetheine arm of dpCoA, such as hydrogen-bonding contacts mediated by the side chains of Lys41, Ser9, Asn38 and Glu132 as well as hydrophobic contacts to Leu 73, Met101 and Leu129, in addition to several water-mediated hydrogen bonds at the PPAT active site (Figures 3A & 4).

The fragments were further characterized by isothermal titration calorimetry. The thermodynamics of the fragment-binding events showed that many were associated with very low heat changes, which may be attributed to a lower enthalpic contribution to binding, as previously reported for *Mtb* PPAT-ATP, where interactions are likely driven by entropic component of displacement of water molecules in the active site[80]. For fragment interactions that resulted in a reasonable binding isotherm, the measured dissociation constants were greater than or equal to 500μM (example shown in Figure 5B), while fragment **2** afforded an average K_d of 66μM (K_d1= 37.3 μM, K_d2 = 83.3 μM, K_d3 = 72.5 μM, K_d4 = 76.3 μM, K_d5 =13.9 μM and K_d6 = 114 μM), where the data were fitted using a six-site sequential binding model (Figure 5C). Interestingly, fragment **2** adopts a dual binding mode where two molecules each of the fragment bind to each subunit of PPAT hexamer, at sub-pockets **I** and **II** respectively (Figures 3D & 4B).

ACCEPTED MANUSCRIPT

Fragment Binding & Hotspot Maps

We further analyzed the binding propensities of PPAT protein to ligands with the help of the hotspot-mapping program developed by Radoux and co-workers [81]. Hotspots are often defined as areas within the protein that provide relatively large contributions to the overall binding affinity of ligands[82, 83]. These regions not only satisfy the minimum binding requirement for fragments but also maintain the original fragment binding interactions when elaborated. The importance of hydration thermodynamics is becoming increasingly recognized as a driving force for fragment binding to target proteins[84]. It has been hypothesized that hotspot regions are characterized by the presence of water molecules having restricted translational and rotational freedom owing to their location within a hydrophobic cavity or close to a patchwork of hydrogen bonds and lipophilic amino-acid sidechains. Ligand binding that displaces such water molecules leads to a favorable free-energy change mainly due to an entropic contribution [84]. The hotspot-mapping program identifies interactions that drive fragment binding by a global search of the protein structure, calculating grid-based atomic propensities for specific donor, acceptor and hydrophobic interactions. This is followed by weighting the propensity scores based on buriedness of the grid points and sampling of the weighted atomic scores using three simple molecular probes to create corresponding donor, acceptor and hydrophobic hotspot maps[81].

While the observed fragment hits satisfy many of the predicted protein-hotspot interactions, the map contoured at a lower level suggests potential ways to elaborate the fragments to reach those hotspot regions that are not yet explored (Figure 5A). For example, fragment **2** is found to be mediating the donor and acceptor hotspots via hydrogen bonds to backbone carbonyl of Gly88 by the indazole NH and to active site Ser9 and Phe10 via the carboxylic acid moiety, at sub-pockets **I** and **II** respectively. Similarly, fragment **4** is found to satisfy the predicted H-bond acceptor interactions through the mandelic acid moiety forming H-bond to Ser9 and active site water molecules and the phenoxy group of the fragment making hydrophobic contact to Leu73. These fragments may be further elaborated in the direction of the hotspots corresponding to interactions with Asn105, Thr113 and Glu98 at the base of the active site, as shown in Figure 5A.

ACCEPTED MANUSCRIPT

'Fragment-like' Drugs against *Mycobacterial species*

Many critical drugs in current chemotherapy regimen against *Mtb* are indeed smaller than 'drug-like' having molecular weights in the range of 100-300 daltons. These include anti-tuberculosis drugs like isoniazid (INH), ethionamide (ETH) and para-aminosalicylic acid (PAS), which are still found to be useful against drug-susceptible TB, as well as pyrazinamide (PZA) a key relapse-reducing drug. Though these drugs require fairly long treatment periods and are less effective against drug-resistant *Mtb*, it is intriguing how these small molecules have retained their killing effect over nearly a century from the time they were developed. Gopal et al[85] in a recent review suggest that molecules that are small, reactive and promiscuous have certain advantages over larger, single-target drugs that may render these molecules effective against mycobacterial species. Compounds like INH, ETH and PZA for example, owing to their small size and promiscuity are more likely to be accepted as substrate analogues and metabolized by bacterial enzymes turning these prodrugs into more reactive compounds capable of hitting multiple-targets, resulting in irreversible damage to the cell. Being small (MW<300Da) and moderately lipophilic (clogP <3) also allows easy penetration of these molecules through the otherwise highly impermeable mycobacterial cell envelope, leading to higher *in-vivo* exposure and favorable pharmacokinetic properties[86, 87] [85].

Based on this idea, Moreira and co-workers in a recent study[88] identified 38 fragment hits having bactericidal activity against *Mtb* (MIC_{50}< 500 μM), from screening a fragment library of 1725 compounds. Interestingly, 23 out of the 38 identified hits were shown to have bactericidal activity against *M. avium* and 13 hits against *Mab* as well. These hits retained their favourable pharmacokinetic properties and a good fraction of the hits were found to be selective against mammalian cells, though no structure-activity relationship could be established.

Fragment-like molecules were found to potentiate the effect of ethionamide (ETH), a second line TB drug, by 10-fold and showed significant intrinsic bactericidal activity in the absence of ethionamide in a study done by Nikiforov and co-workers[89]. Here, Fragment **1** (MEC = 3 ± 1.8 μM) was identified from screening an in-house library of 1250 fragments against *Mtb* EthR using a cascade of biochemical, biophysical and structural biology approaches. EthR, a transcriptional repressor belonging to TetR family, controls the expression of Flavin-dependent, monooxygenase enzyme EthA which in turn activates ethionamide., a second-line anti-TB drug.

ACCEPTED MANUSCRIPT

Subsequent structure activity relationship (SAR) exploration around fragment **1** and its analogue **2** led to the development of the potent ethionamide boosters, the amide **14** (MEC = 0.4 ± 0.2 μM) and the carbamate **28** (MEC = 0.4 ± 0.2 μM), which represent approximately 7-fold improvement in boosting the effect of ethionamide in *Mtb* culture from the starting fragment **1** (MEC = 3 ± 1.8 μM). Further, compounds **14** and **28** showed significant intrinsic bactericidal effect in the absence of ethionamide with (IC50 ≈ 1 μM) and exhibited low nanomolar activity in macrophage assays in the presence of ethionamide[89].

Chemical Elaboration of Fragments for *M. tuberculosis*

For the second stage of FBDD involving elaboration of fragments by growing, merging or linking strategies, we seek to develop a structure-guided approach using the range of biochemical, structural, thermodynamics and kinetic methods. Chemical optimization of fragments involves an iterative process where analysis of binding interactions as well as biophysical, *in-vitro* and *in-vivo* functional testing of the optimized analogues are done to inform further chemical modifications until a significantly potent lead compound is obtained.

Because the fragment-elaboration for the *Mab* PPAT target is ongoing, we use examples of the fragment-merging approach that was successfully applied in our lab and elsewhere to develop small molecule inhibitors of *Mtb*.

(i) Fragment merging to develop inhibitors against *Mtb* EthR.

A fragment-merging approach to develop small molecule inhibitors of *Mtb* EthR led to the development of a potent lead candidate in a recent study[90]. EthR is a physiological dimer having a large hydrophobic binding cavity but containing a number of H-bond acceptors and aromatic residues capable of directed π interactions; the starting fragments **1** & **2** were each found to occupy two distinct sites thus filling the entire cavity as shown in Figure 6A & B. Merging of Fragments **1 & 2** further resulted in a significantly potent lead molecule, compound **15** (Figure 6C) affording an IC_{50} of 3μM[90].

ACCEPTED MANUSCRIPT

(ii) Fragment elaboration to inhibit a *Mtb* cytochrome P450 (CYP) enzyme

A fragment elaboration approach by Hudson & co-workers led to the development of high affinity ligands against CYP121, a cytochrome P450 (CYP) enzyme[91]. The mycobacterial genome encodes for at least 20 different CYPs that play an important role in virulence and survival of the bacteria[92]. CYPs belong to a family of mono-oxygenase enzymes containing heme as a co-factor that catalyze the oxidation of organic molecules and thereby mediate diverse metabolic processes. CYP121 is found exclusively in *Mtb* and helps in the production of mycocyclosin, a secondary metabolite, by catalyzing the formation of a C-C bond between the two tyrosine residues of the substrate cyclodityrosine (cYY). Rv2276, the gene encoding for CYP121, was found to be an essential *Mtb* gene, suggesting that the product mycocyclosin has an important cellular role or an overproduction of the substrate cYY is toxic to the organism[93, 94]. A fragment screening approach that combines fluorescence-based thermal shift assay, NMR (STD and WaterLOGSY) and X-ray crystallography helped in the identification of 4 hits from a fragment library of 665 compounds adopting two distinct binding modes[95].

Elaboration of these fragments hits resulted in several promising derivatives (Figure 6D). In particular, the two different binding conformations of fragment **10** (K_d =1.7mM) was exploited to synthesize compound **12.** Although this was less active than the starting fragment, further replacement of its five-membered ring with an aminopyrazole led to compound **13** with a K_d of 40 μM. Growth of compound **13** into the water-filled cavity of CYP121 resulted in compound **14**, with an additional phenol ring which mediated further H-bonds with the active site water molecules, improving the affinity by over 100-fold from the starting fragment (K_d of 15 μM,)[91, 95, 96]. Elaboration of the lead compound **14** by Kavanagh and colleagues and the addition of a 3amino-phenyl group at the meta position of the aromatic ring attached to five-membered ring, led to compound **15** (K_d of 0.015μM, LE=0.41), the highest affinity inhibitor of CYP121 to date as shown in Figure 6D [97].

ACCEPTED MANUSCRIPT

(iii) Inhibiting *Mtb* Thymidylate kinase

Thymidylate kinase (TMK) is an enzyme that belongs to the DNA synthesis pathways and that produces thymidine 5'-diphosphate using ATP and thymidine 5'-monophosphate. This enzyme is an established drug target and has been the focus for many drug discovery campaigns against different pathogens, in both eukaryotes[98] and prokaryotes, including *Mtb*[99, 100] and also viruses[101]. The essentiality of this enzyme is established in *Mtb* and drug discovery efforts with this target identified a number of inhibitors some of them with active in cell based assays. However, the vast majority of the compounds obtained are analogues of thymidine and contain a thymidine moiety[100]. To move away from these scaffolds, Naik and colleagues carried out a fragment screening of TMK, combining biochemical assay and NMR, which resulted in the identification of a 3-cyanopyridone containing fragment for chemical elaboration[102]. The mode of binding of this fragment hit was determined by molecular docking. Subsequent development of the fragment, supported by X-ray crystal structures of key compounds, allowed the development of nanomolar-potency lead compounds against TMK that retained high ligand efficiency. These compounds were found to have different binding modes from the substrate analogues and some were found to inhibit *Mtb* in whole cell assays.

CONCLUSIONS

The use of protein structure, defined by experimental and computational approaches for renin and HIV protease, developed for target identification, validation and development of new leads in the 1980s and 1990s, has provided a paradigm for use of structural biology to underpin drug discovery. The progress in structure-guided drug discovery has been impressive, but there remain many challenges for the future. They lie not only in more efficient exploration of biological and chemical space at the molecular level, but also in understanding the many aspects of cell and whole organism biology that affect ligand transport, permeability and metabolism, as well as the changes in complex assemblies over space and time.

Progress in defining biological space requires more efficient approaches to improve experimental structures. This may come from X-ray methods using conventional crystallisation techniques and from X-ray small angle scattering. However, some of the most exciting new developments have come from single-particle cryo-EM methods, for example those developed with the new powerful electron microscopes

ACCEPTED MANUSCRIPT

such as the FEI Titan Krios transmission electron microscope (TEM) combined with direct electron detectors[103], and new software such as RELION[104], which carries out 2D image classification followed 3D reconstruction. These revolutionary changes have allowed binding of antibiotics to be envisaged on ribosome particles[105] [106]. This approach will be particularly powerful at defining structures of the complex systems involved in cell regulation and signalling, where interfacial inhibitors or stabilisers are of interest.

Experimental methods of defining biological and chemical space will likely continue to be challenging even for organisms with relatively small genomes. Structures are required to define interactions of macromolecular and small ligands with proteins. The impacts of strain variation, including mutations that are selectively advantageous in evolution as well as disadvantageous in disease, will need to be understood at the level of protein structure. Thus, it is inevitable that computational methods will need to be improved not only to predict the structures and dynamics of monomers and their interactions with small molecules, but also the multicomponent systems often involving proteins that are intrinsically disordered in parts or the whole of their polypeptide chains; these are still very challenging.

As we have seen, fragment-based drug discovery has improved the exploration of chemical space, especially where targets are well described in terms of structure. Fragments that are stably bound and maintain their positions during elaboration bind at hotspots. Some progress has been made in recognising these from the structure as we have described, for example Radoux et al., 2016 [81]. It is now becoming clear that there is wide range of interaction types in addition to H-bonds and simple lipophilic interactions, including π - π , π - δ -positive and π - δ -negative charge, and these can be displayed using software such as Arpeggio [107] & Intermezzo [Ochoa-Montaño, B., Blundell, T.L., unpublished].

Fragment-based approaches have proved successful in getting drugs to the market in cancer, and the lessons learnt are proving helpful in the design of antimicrobials, as we have described. The FBDD approach allows efficient exploration of the chemical space against targets like those of mycobacteria, where features, such as the bacterial cell wall, demand the investigation of molecules that are likely different - in size, lipophilicity and other properties - than those optimised for human protein targets.

Advances in protein crystallography using high-throughput, roboticized approaches at synchrotrons offer further opportunities. Frank von Delft and colleagues have developed automated methods to soak crystals with fragments and mount them in the

ACCEPTED MANUSCRIPT

X-ray beam. Perhaps the most impressive advance has been in PanDDA[108], a method that reveals subtle differences when the ligand is partially occupied. The PanDDA method reveals electron density for only the changed state, even from poor models and inaccurate maps, by subtracting a proportion of the apo state, accurately estimated by averaging many apo-protein crystals.

Fragment based approaches can screen a vast chemical space using a relatively small library of fragments with a set of desired physiochemical properties that can be retained and controlled during the structure-guided optimization of the fragment hits. Finding inhibitors against mycobacteria is a highly challenging task due to the impermeability of cell wall, multidrug efflux-pumps and drug modifying enzymes that these organisms possess. Small hydrophilic molecules are known to cross the mycobacterial cell wall through porins but large macrocycles and small hydrophobic molecules also diffuse through the cell wall, resulting in TB drugs being widely distributed across chemical space[109]. Solving the structure of efflux pumps in these organisms will surely provide insights into the efflux mechanisms and help identify chemical scaffolds that are extruded from cells, thereby allowing FBDD approaches to optimise the chemistry of new lead molecules.

The structure-guided fragment-based approach avoids the requirement for large screening libraries and provides a route to the discovery of new therapeutics for diseases that lead to many deaths throughout the world and gives hope for effective medicines for rare diseases and those that affect the large populations of less affluent parts of the world. Knowledge of protein structure has contributed to the development of early stages of drug discovery and is widely exploited in both industry and academia.

Acknowledgements: We thank Dr.Andres Floto and team for kindly providing *M.abcessus* genomic DNA. Prof. Chris Abell and Dr.Anthony Coyne for access to the in-house fragment library collection. The authors would like to thank Diamond Light Source for beam-time (proposals mx9537, mx14043) and the staff of beamlines I03, I04, I04-1 and I24 for assistance with data collection. SET is funded by the Cystic Fibrosis Trust (Registered as a charity in England and Wales (1079049) and in Scotland (SC040196); VM and BOM are funded by the Bill and Melinda Gates Foundation; SM is funded by the Medical Research Council (MRC Newton/DBT Grant: RG78439); TLB is funded by the Wellcome Trust (Wellcome Trust Investigator Award: 200814/Z/16/Z).

ACCEPTED MANUSCRIPT

ACCESSION NUMBERS: Coordinates and structure factors have been deposited in the Protein Data Bank with accession numbers: 5O06; 5O08; 5O0A; 5O0B; 5O0C; 5O0D; 5O0F; 5O0H.

Figure Legends:

Figure 1: A) Schematic to illustrate the concept of drug discovery by exploring biological space encompassing genome information to identify new targets, followed by exploration of chemical space using screening libraries based on knowledge of the target. Target protein in the illustration: HIV-1 proteinase (PDB code: 3PHV), Drug: HIV proteinase inhibitor: saquinavir (Roche) **B)** Fragment Based Drug Discovery workflow illustrated as four stages involving 1.Target Identification and protein production 2.Fragment library screening 3. Hit validation and 4. Iterative fragment elaboration cycle through to a potential lead candidate. Various tools and techniques involved at each stage of the process are also shown.

Figure 2: A) Schematic depicting bacterial Coenzyme A biosynthetic pathway. The penultimate step catalyzed by PPAT enzyme is boxed and the gene names corresponding to each enzyme is given in brackets. Many organisms are capable of exogenous uptake of the starting substarte Pantothenate, while some bacteria and fungi undertake de-novo Pantothenate synthesis from β-alanine and Pantoate, catalysed by Pantothenate synthetase (panC). PPCS* and PPCDC* activities residue within a single polypeptide chain in bacteria. **B)** Crystal structure of *Mab* PPAT:Apo solved at 1.5Å resolution showing a hexameric assembly. **C)** Protomer of *Mab* PPAT bound to dpCoA (purple ball & stick representation) forming a 'bent' conformation at active site. The secondary structure elements are coloured with β-strands in yellow, α- helices in red and loop regions in green. **D)** Structural superposition of *Mab* PPAT:Apo (green) and *Mab* PPAT:dpCoA (blue) at C^{α} atoms showing conformational changes in the flexible loop II and loop IV. dpCoA, represented as spheres, is seen bound to all the three protomers in the asymmetric unit. **E)** Enlarged view showing conformational changes at loop II positioning the invariant catalytic Lys41 residue close to adenylyl α-phosphate of dpCoA (shown in pink stick representation) and ordering of loop IV to two complete α-helical turns at the N-terminal of helix4 at the base of catalytic site along with inward flipping of the Arg90. Other invariant residues interacting with DpCoA, His17 and Ser9 are also shown. The figures were prepared using Pymol (PyMOL Molecular Graphics System, Version 1.7 Schrödinger, LLC). PDB codes: *Mab* PPAT:Apo: 5O06, *Mab* PPAT:dpCoA: 5O08.

ACCEPTED MANUSCRIPT

Figure 3: A) Active site diagram showing binding interactions of dpCoA shown in pink ball and stick model and the active site residues as green lines. Hydrogen bonds are represented with blue dotted lines, π-interactions in black dotted lines, hydrophobic contacts in red dotted lines**. B)** Overlay of *Mab* PPAT:Apo (green) and *Mab* PPAT: fragment **1**(orange) structures showing conformational changes in loop IV invariant Arg90, His17 and Ser127 are represented in blue lines. **D & C)** Structural Superposition of six Mab PPAT structures bound to fragments **1**(purple), **2**(gold), **3**(green), **4**(blue), **5**(salmon) and **6**(turquoise), showing fragments occupying four distinct regions (**I-IV**) in the PPAT active site shown in surface electrostatic representation. (PDB codes: 5O0A, 5O0B, 5O0C, 5O0D, 5O0F, 5O0H).The figures were prepared using Pymol (PyMOL Molecular Graphics System, Version 1.7 Schrödinger, LLC) and Intermezzo (Ochoa-Montaño, B., Blundell, T.L. et al unpublished; Jubb, H.C., et al, 2017 [105]).

Figure 4: Active site diagram of *Mab* PPAT showing binding interactions of fragments **1-6 (**shown in orange ball and stick model) from A to F respectively and the active site residues as blue lines. Fragment contacts are represented as dotted lines, hydrogen bonds are represented in blue, π-interactions in black, hydrophobic contacts in red and ionic contacts in green dotted lines respectively**.** The figures were prepared using Pymol (PyMOL Molecular Graphics System, Version 1.7 Schrödinger, LLC) and Intermezzo (Ochoa-Montaño, B., Blundell, T.L. et al unpublished; Jubb, H.C. et al, 2017[105]). (PDB codes 5O0A, 5O0B, 5O0C, 5O0D, 5O0F, 5O0H)

Figure 5: A) Hotspot map (Radoux et al, 2015) [79] of *Mab* PPAT:Apo protein with *Mab* PPAT structures bound to fragments **1**(purple), **2**(gold), **3**(green), **4**(blue), **5**(salmon) and **6**(turquoise), overlaid. The hydrophobic hotspot map is shown in yellow, donor and acceptor hotspots are shown as blue and red surfaces respectively. The major residues mediating interactions at the hotspots are shown in white stick representation**. B)** Representative thermodynamic profile for fragment binding to *Mab* PPAT. *The figures were prepared using Pymol (PyMOL Molecular Graphics System, Version 1.7 Schrödinger, LLC). (PDB codes:* 5O0A, 5O0B, 5O0C, 5O0D, 5O0F, 5O0H*)*

ACCEPTED MANUSCRIPT

Figure 6: Fragment elaboration to develop inhibitors of *Mtb.* **A)** Fragment merging approach to develop small molecule inhibitors of *Mtb* EthR. The region corresponding to the hydrophobic binding cavity of EthR dimer is boxed. **B)** binding pocket of EthR where the starting fragments **1** (in gold) & **2** (in grey) were each found to occupy two distinct sites in two copies thereby filling the entire cavity involving sub-pockets **I, II, II** and **IV** (marked in blue) **C)** Merging of Fragments **1** (in gold) & **2** (in grey) results in a significantly potent lead, compound **15** (green). The corresponding thermal shift and IC_{50}values for each compound are also illustrated. PDB codes: 5FIJ, 5F27, 5F0F. **D)** Fragment elaboration to develop compounds that inhibit *Mtb* CYP121. Two molecules of Fragment **10** (green) binds CYP121 near the Heme (yellow) binding pocket. Subsequent merging and elaboration of fragment **10**, via compounds **13** and **14 (blue)**, led to the development of potent compound **15 (pink).** The corresponding K_d and Ligand efficiency values for each compound are also illustrated. PDB codes (4G47, 4KTL, 5IBE). The figures were prepared using Pymol (PyMOL Molecular Graphics System, Version 1.7 Schrödinger, LLC).

ACCEPTED MANUSCRIPT

ACCEPTED MANUSCRIPT

References

[1] Perutz RR, Liquori AM, Eirich F. X-ray and solubility studies of the haemoglobin of sickle-cell anaemia patients. Nature. 1951;167:929-31.
[2] Perutz MF, Rossmann MG, Cullis AF, Muirhead H, Will G, North AC. Structure of haemoglobin: a three-dimensional Fourier synthesis at 5.5-A. resolution, obtained by X-ray analysis. Nature. 1960;185:416-22.
[3] Kendrew JC, Dickerson RE, Strandberg BE, Hart RG, Davies DR, Phillips DC, et al. Structure of myoglobin: A three-dimensional Fourier synthesis at 2 A. resolution. Nature. 1960;185:422-7.
[4] Schlichtkrull JEM. Insulin Crystals: Chemical & Biological Studies on Insulin Crystals & Insulin Zinc Suspensions Ejnar Munksggard, Copenhagen
; 1958.
[5] Adams MJ, Blundell TL, Dodson EJ, Dodson GG, Vijayan M, Baker EN, et al. Structure of Rhombohedral 2 Zinc Insulin Crystals. Nature. 1969;224:491-5.
[6] Blundell TL, Cutfield JF, Cutfield SM, Dodson EJ, Dodson GG, Hodgkin DC, et al. Atomic positions in rhombohedral 2-zinc insulin crystals. Nature. 1971;231:506-11.
[7] Sanger F. Sequences, sequences, and sequences. Annu Rev Biochem. 1988;57:1-28.
[8] Beddell CR, Goodford PJ, Norrington FE, Wilkinson S, Wootton R. Compounds designed to fit a site of known structure in human haemoglobin. Br J Pharmacol. 1976;57:201-9.
[9] Skeggs LT, Dorer, F. E., Levine, M., Lentz, K. E. & Kahn, J. R. The Renin-Angiotensin System In: Johnson JAA, R. R., editor.: Plenum, New York; 1980. p. 1-27.
[10] Atkinson AB. The Therapeutics of Hypertension. Academic and The Royal Society of Medicine, London; 1980. p. 29–61.
[11] James MN, Hsu IN, Delbaere LT. Mechanism of acid protease catalysis based on the crystal structure of penicillopepsin. Nature. 1977;267:808-13.
[12] Subramanian E, Swan ID, Liu M, Davies DR, Jenkins JA, Tickle IJ, et al. Homology among acid proteases: comparison of crystal structures at 3A resolution of acid proteases from Rhizopus chinensis and Endothia parasitica. Proceedings of the National Academy of Sciences of the United States of America. 1977;74:556-9.
[13] Tickle IJ, Sibanda, B.L., Pearl, L.H., Hemmings, A.M. & Blundell, T.L. . Protein crystallography, interactive computer graphics & drug design X-ray Crystallography & Drug Design. Clarendon Press, Oxford, UK, ; 1984. p. 427-44.
[14] Blundell T, Sibanda BL, Pearl L. Three-dimensional structure, specificity and catalytic mechanism of renin. Nature. 1983;304:273-5.
[15] Rahuel J, Priestle JP, Grutter MG. The crystal structures of recombinant glycosylated human renin alone and in complex with a transition state analog inhibitor. Journal of structural biology. 1991;107:227-36.
[16] Dhanaraj V, Dealwis CG, Frazao C, Badasso M, Sibanda BL, Tickle IJ, et al. X-ray analyses of peptide-inhibitor complexes define the structural basis of specificity for human and mouse renins. Nature. 1992;357:466-72.
[17] Tang J, James MN, Hsu IN, Jenkins JA, Blundell TL. Structural evidence for gene duplication in the evolution of the acid proteases. Nature. 1978;271:618-21.
[18] Hiroyuki Toh MO, Kaoru Saigo & Takashi Miyata. Retroviral protease-like sequence in the yeast transposon Ty 1. Nature

ACCEPTED MANUSCRIPT

. 1985;315.
[19] Pearl LH, Taylor WR. A structural model for the retroviral proteases. Nature. 1987;329:351-4.
[20] Jaskolski M, Miller M, Rao JK, Leis J, Wlodawer A. Structure of the aspartic protease from Rous sarcoma retrovirus refined at 2-A resolution. Biochemistry. 1990;29:5889-98.
[21] Jaskolski M, Miller, M., Rao, M., Leis, J., Wlodawer, A., Leis, J. P. Structure of the aspartic protease from Rous sarcoma virus at 2A resolution. In: Krausslich H, Oroszlan, S., Wimmer, E., editor. Current Communications in Molecular Biology: Cold Spring Harbor Press; 1989.
[22] Navia MA, Fitzgerald PM, McKeever BM, Leu CT, Heimbach JC, Herber WK, et al. Three-dimensional structure of aspartyl protease from human immunodeficiency virus HIV-1. Nature. 1989;337:615-20.
[23] Blundell T, Pearl L. Retroviral proteinases. A second front against AIDS. Nature. 1989;337:596-7.
[24] Wlodawer A, Miller M, Jaskolski M, Sathyanarayana BK, Baldwin E, Weber IT, et al. Conserved folding in retroviral proteases: crystal structure of a synthetic HIV-1 protease. Science. 1989;245:616-21.
[25] Lapatto R, Blundell T, Hemmings A, Overington J, Wilderspin A, Wood S, et al. X-ray analysis of HIV-1 proteinase at 2.7 A resolution confirms structural homology among retroviral enzymes. Nature. 1989;342:299-302.
[26] Jaskolski M, Dauter Z, Wlodawer A. A brief history of macromolecular crystallography, illustrated by a family tree and its Nobel fruits. FEBS J. 2014;281:3985-4009.
[27] Bohacek RS, McMartin C, Guida WC. The art and practice of structure-based drug design: a molecular modeling perspective. Med Res Rev. 1996;16:3-50.
[28] Murray CW, Erlanson DA, Hopkins AL, Keseru GM, Leeson PD, Rees DC, et al. Validity of ligand efficiency metrics. ACS medicinal chemistry letters. 2014;5:616-8.
[29] Harner MJ, Frank AO, Fesik SW. Fragment-based drug discovery using NMR spectroscopy. Journal of biomolecular NMR. 2013;56:65-75.
[30] Murray CW, Verdonk ML, Rees DC. Experiences in fragment-based drug discovery. Trends in pharmacological sciences. 2012;33:224-32.
[31] Blundell TL, Jhoti H, Abell C. High-throughput crystallography for lead discovery in drug design. Nat Rev Drug Discov. 2002;1:45-54.
[32] Scott DE, Coyne AG, Hudson SA, Abell C. Fragment-based approaches in drug discovery and chemical biology. Biochemistry. 2012;51:4990-5003.
[33] Niesen FH, Berglund H, Vedadi M. The use of differential scanning fluorimetry to detect ligand interactions that promote protein stability. Nature protocols. 2007;2:2212-21.
[34] Navratilova I, Hopkins AL. Fragment screening by surface plasmon resonance. ACS medicinal chemistry letters. 2010;1:44-8.
[35] Taylor RD, MacCoss M, Lawson AD. Combining Molecular Scaffolds from FDA Approved Drugs: Application to Drug Discovery. Journal of medicinal chemistry. 2017;60:1638-47.
[36] Abagyan R, Totrov M. High-throughput docking for lead generation. Current opinion in chemical biology. 2001;5:375-82.
[37] Hubbard RE, Murray JB. Experiences in fragment-based lead discovery. Methods in enzymology. 2011;493:509-31.

ACCEPTED MANUSCRIPT

[38] Winter A, Sigurdardottir AG, DiCara D, Valenti G, Blundell TL, Gherardi E. Developing Antagonists for the Met-HGF/SF Protein-Protein Interaction Using a Fragment-Based Approach. Molecular cancer therapeutics. 2016;15:3-14.
[39] World Health Organization, Global tuberculosis report. 2016.
[40] Wallis RS, Maeurer M, Mwaba P, Chakaya J, Rustomjee R, Migliori GB, et al. Tuberculosis--advances in development of new drugs, treatment regimens, host-directed therapies, and biomarkers. The Lancet Infectious diseases. 2016;16:e34-46.
[41] Marras TK, Mendelson D, Marchand-Austin A, May K, Jamieson FB. Pulmonary nontuberculous mycobacterial disease, Ontario, Canada, 1998-2010. Emerging infectious diseases. 2013;19:1889-91.
[42] Lai CC, Tan CK, Chou CH, Hsu HL, Liao CH, Huang YT, et al. Increasing incidence of nontuberculous mycobacteria, Taiwan, 2000-2008. Emerging infectious diseases. 2010;16:294-6.
[43] Qvist T, Pressler T, Hoiby N, Katzenstein TL. Shifting paradigms of nontuberculous mycobacteria in cystic fibrosis. Respiratory research. 2014;15:41.
[44] Bryant JM, Grogono DM, Greaves D, Foweraker J, Roddick I, Inns T, et al. Whole-genome sequencing to identify transmission of Mycobacterium abscessus between patients with cystic fibrosis: a retrospective cohort study. Lancet. 2013;381:1551-60.
[45] Nessar R, Cambau E, Reyrat JM, Murray A, Gicquel B. Mycobacterium abscessus: a new antibiotic nightmare. The Journal of antimicrobial chemotherapy. 2012;67:810-8.
[46] Griffith DE, Aksamit T, Brown-Elliott BA, Catanzaro A, Daley C, Gordin F, et al. An official ATS/IDSA statement: diagnosis, treatment, and prevention of nontuberculous mycobacterial diseases. American journal of respiratory and critical care medicine. 2007;175:367-416.
[47] Lee MR, Sheng WH, Hung CC, Yu CJ, Lee LN, Hsueh PR. Mycobacterium abscessus Complex Infections in Humans. Emerging infectious diseases. 2015;21:1638-46.
[48] Parkins MD, Floto RA. Emerging bacterial pathogens and changing concepts of bacterial pathogenesis in cystic fibrosis. Journal of cystic fibrosis : official journal of the European Cystic Fibrosis Society. 2015;14:293-304.
[49] Bar-On O, Mussaffi H, Mei-Zahav M, Prais D, Steuer G, Stafler P, et al. Increasing nontuberculous mycobacteria infection in cystic fibrosis. Journal of cystic fibrosis : official journal of the European Cystic Fibrosis Society. 2015;14:53-62.
[50] Heydari H, Wee WY, Lokanathan N, Hari R, Mohamed Yusoff A, Beh CY, et al. MabsBase: a Mycobacterium abscessus genome and annotation database. PloS one. 2013;8:e62443.
[51] Benwill JL, Wallace RJ, Jr. Mycobacterium abscessus: challenges in diagnosis and treatment. Curr Opin Infect Dis. 2014;27:506-10.
[52] Jarlier V, Nikaido H. Permeability barrier to hydrophilic solutes in Mycobacterium chelonei. J Bacteriol. 1990;172:1418-23.
[53] Nguyen L, Thompson CJ. Foundations of antibiotic resistance in bacterial physiology: the mycobacterial paradigm. Trends in microbiology. 2006;14:304-12.

ACCEPTED MANUSCRIPT

[54] Ripoll F, Pasek S, Schenowitz C, Dossat C, Barbe V, Rottman M, et al. Non mycobacterial virulence genes in the genome of the emerging pathogen Mycobacterium abscessus. PloS one. 2009;4:e5660.
[55] Kothavade RJ, Dhurat RS, Mishra SN, Kothavade UR. Clinical and laboratory aspects of the diagnosis and management of cutaneous and subcutaneous infections caused by rapidly growing mycobacteria. European journal of clinical microbiology & infectious diseases : official publication of the European Society of Clinical Microbiology. 2013;32:161-88.
[56] Ramakrishnan G, Ochoa-Montano B, Raghavender US, Mudgal R, Joshi AG, Chandra NR, et al. Enriching the annotation of Mycobacterium tuberculosis H37Rv proteome using remote homology detection approaches: insights into structure and function. Tuberculosis (Edinb). 2015;95:14-25.
[57] Berman HM, Westbrook J, Feng Z, Gilliland G, Bhat TN, Weissig H, et al. The Protein Data Bank. Nucleic acids research. 2000;28:235-42.
[58] Malhotra S, Thomas SE, Ochoa Montano B, Blundell TL. Structure-guided, target-based drug discovery - exploiting genome information from HIV to mycobacterial infections. Postepy biochemii. 2016;62:262-72.
[59] Geerlof A, Lewendon A, Shaw WV. Purification and characterization of phosphopantetheine adenylyltransferase from Escherichia coli. The Journal of biological chemistry. 1999;274:27105-11.
[60] Abiko Y. Investigations on pantothenic acid and its related compounds. IX. Biochemical studies.4. Separation and substrate specificity of pantothenate kinase and phosphopantothenoylcysteine synthetase. Journal of biochemistry. 1967;61:290-9.
[61] Robishaw JD, Neely JR. Coenzyme A metabolism. The American journal of physiology. 1985;248:E1-9.
[62] Izard T, Geerlof A. The crystal structure of a novel bacterial adenylyltransferase reveals half of sites reactivity. The EMBO journal. 1999;18:2021-30.
[63] Jackowski S, Rock CO. Metabolism of 4'-phosphopantetheine in Escherichia coli. J Bacteriol. 1984;158:115-20.
[64] Gerdes SY, Scholle MD, D'Souza M, Bernal A, Baev MV, Farrell M, et al. From genetic footprinting to antimicrobial drug targets: examples in cofactor biosynthetic pathways. J Bacteriol. 2002;184:4555-72.
[65] Wubben T, Mesecar AD. Structure of Mycobacterium tuberculosis phosphopantetheine adenylyltransferase in complex with the feedback inhibitor CoA reveals only one active-site conformation. Acta crystallographica Section F, Structural biology and crystallization communications. 2011;67:541-5.
[66] Aghajanian S, Worrall DM. Identification and characterization of the gene encoding the human phosphopantetheine adenylyltransferase and dephospho-CoA kinase bifunctional enzyme (CoA synthase). Biochem J. 2002;365:13-8.
[67] Daugherty M, Polanuyer B, Farrell M, Scholle M, Lykidis A, de Crecy-Lagard V, et al. Complete reconstitution of the human coenzyme A biosynthetic pathway via comparative genomics. The Journal of biological chemistry. 2002;277:21431-9.
[68] Zhyvoloup A, Nemazanyy I, Babich A, Panasyuk G, Pobigailo N, Vudmaska M, et al. Molecular cloning of CoA Synthase. The missing link in CoA biosynthesis. The Journal of biological chemistry. 2002;277:22107-10.

ACCEPTED MANUSCRIPT

[69] Zhao L, Allanson NM, Thomson SP, Maclean JK, Barker JJ, Primrose WU, et al. Inhibitors of phosphopantetheine adenylyltransferase. Eur J Med Chem. 2003;38:345-9.
[70] Miller JR, Thanabal V, Melnick MM, Lall M, Donovan C, Sarver RW, et al. The use of biochemical and biophysical tools for triage of high-throughput screening hits - A case study with Escherichia coli phosphopantetheine adenylyltransferase. Chemical biology & drug design. 2010;75:444-54.
[71] de Jonge BL, Walkup GK, Lahiri SD, Huynh H, Neckermann G, Utley L, et al. Discovery of inhibitors of 4'-phosphopantetheine adenylyltransferase (PPAT) to validate PPAT as a target for antibacterial therapy. Antimicrobial agents and chemotherapy. 2013;57:6005-15.
[72] Izard T. The crystal structures of phosphopantetheine adenylyltransferase with bound substrates reveal the enzyme's catalytic mechanism. Journal of molecular biology. 2002;315:487-95.
[73] Takahashi H, Inagaki E, Fujimoto Y, Kuroishi C, Nodake Y, Nakamura Y, et al. Structure and implications for the thermal stability of phosphopantetheine adenylyltransferase from Thermus thermophilus. Acta crystallographica Section D, Biological crystallography. 2004;60:97-104.
[74] Badger J, Sauder JM, Adams JM, Antonysamy S, Bain K, Bergseid MG, et al. Structural analysis of a set of proteins resulting from a bacterial genomics project. Proteins. 2005;60:787-96.
[75] Yoon HJ, Kang JY, Mikami B, Lee HH, Suh SW. Crystal structure of phosphopantetheine adenylyltransferase from Enterococcus faecalis in the ligand-unbound state and in complex with ATP and pantetheine. Molecules and cells. 2011;32:431-5.
[76] Edwards TE, Leibly DJ, Bhandari J, Statnekov JB, Phan I, Dieterich SH, et al. Structures of phosphopantetheine adenylyltransferase from Burkholderia pseudomallei. Acta crystallographica Section F, Structural biology and crystallization communications. 2011;67:1032-7.
[77] Chatterjee R, Mondal A, Basu A, Datta S. Transition of phosphopantetheine adenylyltransferase from catalytic to allosteric state is characterized by ternary complex formation in Pseudomonas aeruginosa. Biochimica et biophysica acta. 2016;1864:773-86.
[78] Eventoff W, Rossmann MG. The evolution of dehydrogenases and kinases. CRC critical reviews in biochemistry. 1975;3:111-40.
[79] Timofeev V, Smirnova E, Chupova L, Esipov R, Kuranova I. X-ray study of the conformational changes in the molecule of phosphopantetheine adenylyltransferase from Mycobacterium tuberculosis during the catalyzed reaction. Acta crystallographica Section D, Biological crystallography. 2012;68:1660-70.
[80] Wubben TJ, Mesecar AD. Kinetic, thermodynamic, and structural insight into the mechanism of phosphopantetheine adenylyltransferase from Mycobacterium tuberculosis. Journal of molecular biology. 2010;404:202-19.
[81] Radoux CJ, Olsson TS, Pitt WR, Groom CR, Blundell TL. Identifying Interactions that Determine Fragment Binding at Protein Hotspots. Journal of medicinal chemistry. 2016;59:4314-25.
[82] Hajduk PJ, Huth JR, Fesik SW. Druggability indices for protein targets derived from NMR-based screening data. Journal of medicinal chemistry. 2005;48:2518-25.

ACCEPTED MANUSCRIPT

[83] Hajduk PJ, Huth JR, Tse C. Predicting protein druggability. Drug discovery today. 2005;10:1675-82.
[84] Ichihara O, Shimada Y, Yoshidome D. The importance of hydration thermodynamics in fragment-to-lead optimization. ChemMedChem. 2014;9:2708-17.
[85] Gopal P, Dick T. Reactive dirty fragments: implications for tuberculosis drug discovery. Current opinion in microbiology. 2014;21:7-12.
[86] Barry CE, 3rd, Boshoff HI, Dartois V, Dick T, Ehrt S, Flynn J, et al. The spectrum of latent tuberculosis: rethinking the biology and intervention strategies. Nat Rev Microbiol. 2009;7:845-55.
[87] East SP, Silver LL. Multitarget ligands in antibacterial research: progress and opportunities. Expert Opin Drug Discov. 2013;8:143-56.
[88] Moreira W, Lim JJ, Yeo SY, Ramanujulu PM, Dymock BW, Dick T. Fragment-Based Whole Cell Screen Delivers Hits against M. tuberculosis and Non-tuberculous Mycobacteria. Frontiers in microbiology. 2016;7:1392.
[89] Nikiforov PO, Blaszczyk M, Surade S, Boshoff HI, Sajid A, Delorme V, et al. Fragment-sized EthR inhibitors exhibit exceptionally strong ethionamide boosting effect in whole cell Mycobacterium tuberculosis assays. ACS chemical biology. 2017.
[90] Nikiforov PO, Surade S, Blaszczyk M, Delorme V, Brodin P, Baulard AR, et al. A fragment merging approach towards the development of small molecule inhibitors of Mycobacterium tuberculosis EthR for use as ethionamide boosters. Organic & biomolecular chemistry. 2016;14:2318-26.
[91] Hudson SA, McLean KJ, Surade S, Yang YQ, Leys D, Ciulli A, et al. Application of fragment screening and merging to the discovery of inhibitors of the Mycobacterium tuberculosis cytochrome P450 CYP121. Angew Chem Int Ed Engl. 2012;51:9311-6.
[92] Cole ST, Brosch R, Parkhill J, Garnier T, Churcher C, Harris D, et al. Deciphering the biology of Mycobacterium tuberculosis from the complete genome sequence. Nature. 1998;393:537-44.
[93] Belin P, Le Du MH, Fielding A, Lequin O, Jacquet M, Charbonnier JB, et al. Identification and structural basis of the reaction catalyzed by CYP121, an essential cytochrome P450 in Mycobacterium tuberculosis. Proceedings of the National Academy of Sciences of the United States of America. 2009;106:7426-31.
[94] McLean KJ, Carroll P, Lewis DG, Dunford AJ, Seward HE, Neeli R, et al. Characterization of active site structure in CYP121. A cytochrome P450 essential for viability of Mycobacterium tuberculosis H37Rv. The Journal of biological chemistry. 2008;283:33406-16.
[95] Hudson SA, McLean KJ, Munro AW, Abell C. Mycobacterium tuberculosis cytochrome P450 enzymes: a cohort of novel TB drug targets. Biochemical Society transactions. 2012;40:573-9.
[96] Hudson SA, Surade S, Coyne AG, McLean KJ, Leys D, Munro AW, et al. Overcoming the limitations of fragment merging: rescuing a strained merged fragment series targeting Mycobacterium tuberculosis CYP121. ChemMedChem. 2013;8:1451-6.
[97] Kavanagh ME, Coyne AG, McLean KJ, James GG, Levy CW, Marino LB, et al. Fragment-Based Approaches to the Development of Mycobacterium tuberculosis CYP121 Inhibitors. Journal of medicinal chemistry. 2016;59:3272-302.

ACCEPTED MANUSCRIPT

[98] Noguchi Y, Yasuda Y, Tashiro M, Kataoka T, Kitamura Y, Kandeel M, et al. Synthesis of carbocyclic pyrimidine nucleosides and their inhibitory activities against Plasmodium falciparum thymidylate kinase. Parasitology international. 2013;62:368-71.
[99] Martinez-Botella G, Breen JN, Duffy JE, Dumas J, Geng B, Gowers IK, et al. Discovery of selective and potent inhibitors of gram-positive bacterial thymidylate kinase (TMK). Journal of medicinal chemistry. 2012;55:10010-21.
[100] Van Calenbergh S, Pochet S, Munier-Lehmann H. Drug design and identification of potent leads against mycobacterium tuberculosis thymidine monophosphate kinase. Current topics in medicinal chemistry. 2012;12:694-705.
[101] Guimaraes AP, de Souza FR, Oliveira AA, Goncalves AS, de Alencastro RB, Ramalho TC, et al. Design of inhibitors of thymidylate kinase from Variola virus as new selective drugs against smallpox. Eur J Med Chem. 2015;91:72-90.
[102] Naik M, Raichurkar A, Bandodkar BS, Varun BV, Bhat S, Kalkhambkar R, et al. Structure guided lead generation for M. tuberculosis thymidylate kinase (Mtb TMK): discovery of 3-cyanopyridone and 1,6-naphthyridin-2-one as potent inhibitors. Journal of medicinal chemistry. 2015;58:753-66.
[103] Henderson R. Overview and future of single particle electron cryomicroscopy. Archives of biochemistry and biophysics. 2015;581:19-24.
[104] Scheres SH. RELION: implementation of a Bayesian approach to cryo-EM structure determination. J Struct Biol. 2012;180:519-30.
[105] Brown A, Amunts A, Bai XC, Sugimoto Y, Edwards PC, Murshudov G, et al. Structure of the large ribosomal subunit from human mitochondria. Science. 2014;346:718-22.
[106] Wong W, Bai XC, Brown A, Fernandez IS, Hanssen E, Condron M, et al. Cryo-EM structure of the Plasmodium falciparum 80S ribosome bound to the anti-protozoan drug emetine. eLife. 2014;3.
[107] Jubb HC, Higueruelo AP, Ochoa-Montano B, Pitt WR, Ascher DB, Blundell TL. Arpeggio: A Web Server for Calculating and Visualising Interatomic Interactions in Protein Structures. Journal of molecular biology. 2017;429:365-71.
[108] Pearce NM, Krojer T, Bradley AR, Collins P, Nowak RP, Talon R, et al. A multi-crystal method for extracting obscured crystallographic states from conventionally uninterpretable electron density. Nature communications. 2017;8:15123.
[109] Koul A, Arnoult E, Lounis N, Guillemont J, Andries K. The challenge of new drug discovery for tuberculosis. Nature. 2011;469:483-90.

ACCEPTED MANUSCRIPT

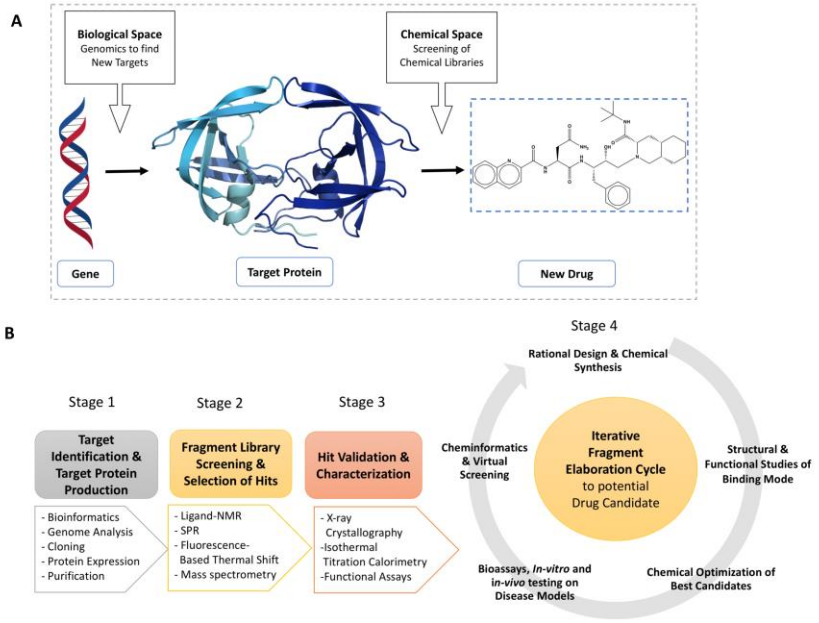

Figure 1

ACCEPTED MANUSCRIPT

ACCEPTED MANUSCRIPT

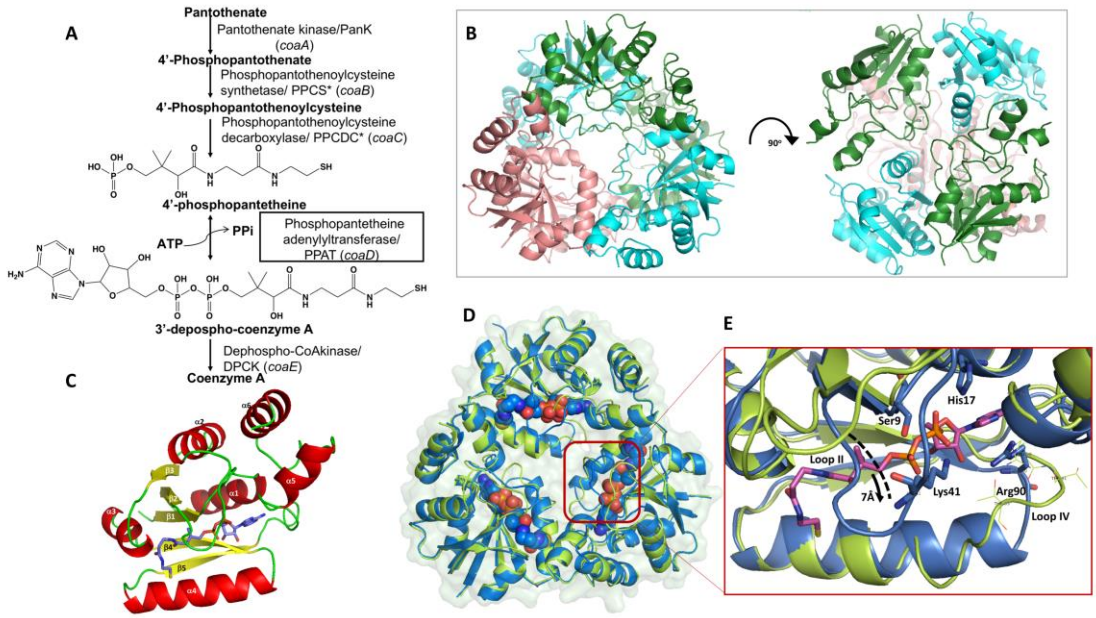

Figure 2

ACCEPTED MANUSCRIPT

ACCEPTED MANUSCRIPT

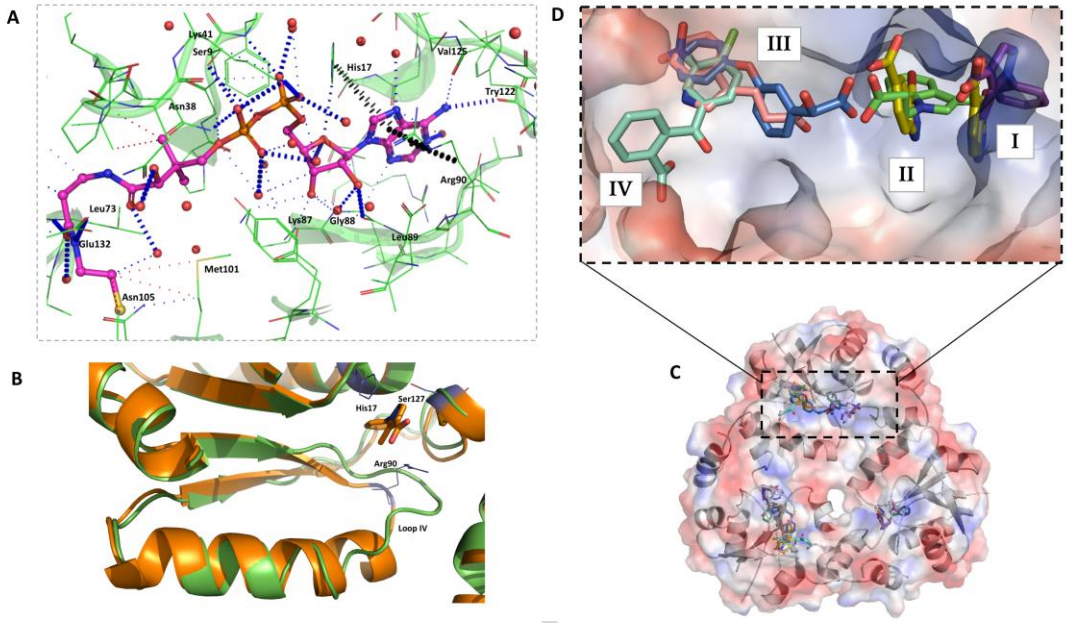

Figure 3

ACCEPTED MANUSCRIPT

ACCEPTED MANUSCRIPT

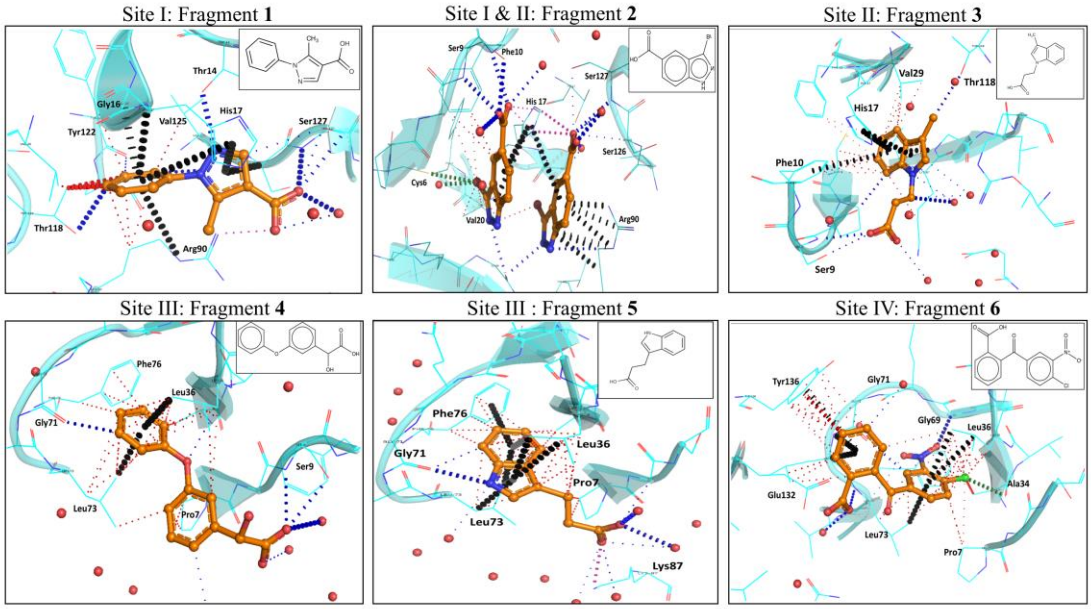

Figure 4

ACCEPTED MANUSCRIPT

ACCEPTED MANUSCRIPT

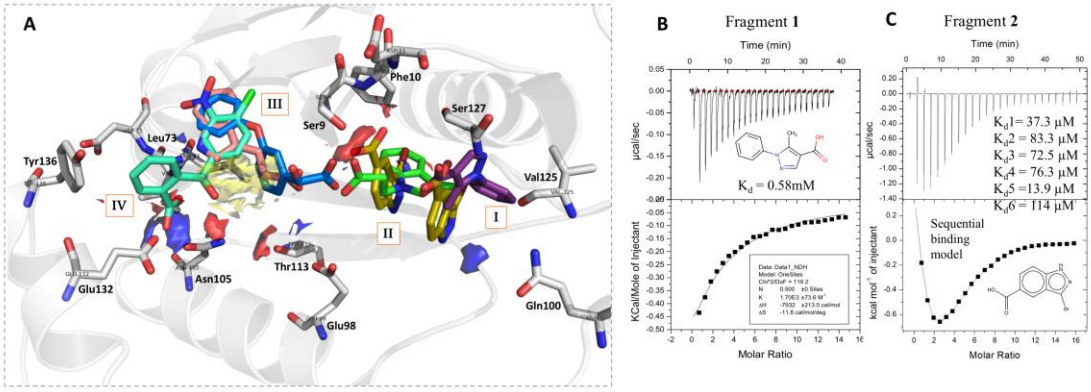

Figure 5

ACCEPTED MANUSCRIPT

ACCEPTED MANUSCRIPT

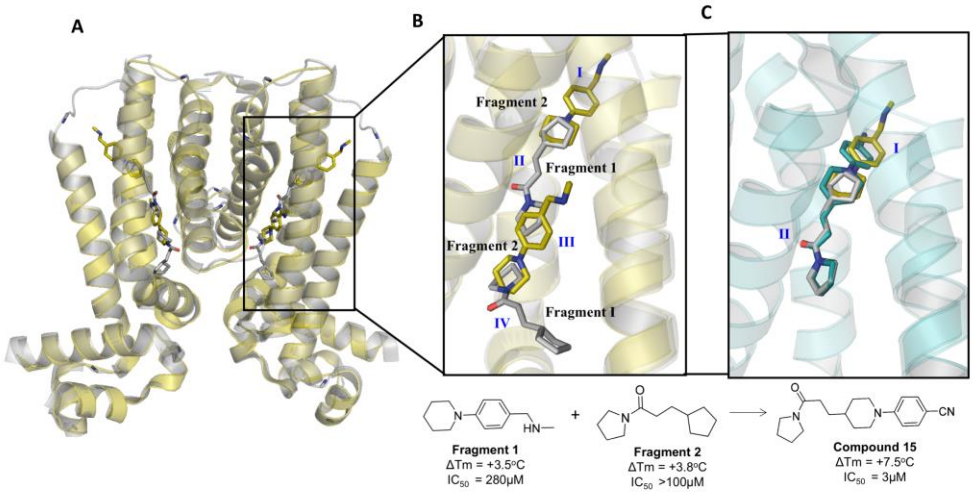

Figure 6 a-c

ACCEPTED MANUSCRIPT

ACCEPTED MANUSCRIPT

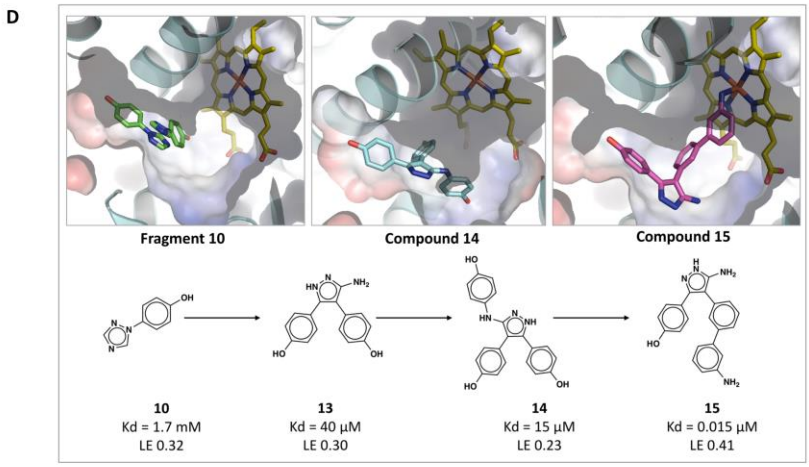

Figure 6 d

ACCEPTED MANUSCRIPT

ACCEPTED MANUSCRIPT

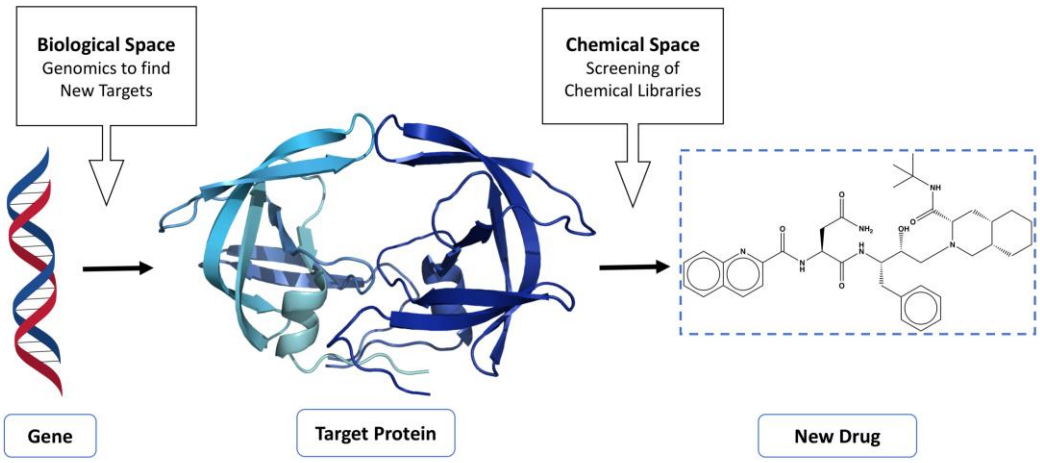

Graphical abstract

ACCEPTED MA